ISSN 2320 2599

Volume 1, No.1, November – December 2012

International Journal of Microwaves Applications

Available Online at http://warse.org/pdfs/ijma01112012.pdf

Analysis and Design of a 12-Element-Coupled-Microstrip-Line TEM Resonator for MRI

NADIA BENABDALLAH[1], NASREDDINE BENAHMED[2], FETHI TARIK BENDIMERAD[2], KAMILA ALIANE[2]

[1] Department of Physics, Preparatory School of Sciences and Technology (EPST-Tlemcen), Tlemcen, Algeria

[2]Department of Telecommunications, University of Tlemcen, P. O. Box 119, (13000) Tlemcen, Algeria

ABSTRACT

The electromagnetic (EM) analysis and design of a n-element unloaded coupled-microstrip-line TEM resonator are presented in this paper by using the finite element method (FEM) and method of moments (MoM) in two dimensions. The analysis allows the determination of the primary inductive and capacitive matrices ([L], [C_0]) and simulates the frequency response of S_{11} at the RF port of the designed n-element unloaded coupled-microstrip-line TEM resonator. As an application, we present the design results of a MRI probe using a 12-element unloaded coupled-microstrip-line TEM resonator and operating at 200 MHz (proton imaging at 4.7 T). The probe has -118 dB minimum reflection and an unloaded quality factor Q_o > 500 at 200 MHz. The twelve-element unloaded coupled-microstrip-line TEM resonator can be designed at any resonance frequency for MRI applications, using the EM parameters values presented into this paper.

Keywords: 12-element unloaded coupled-microstrip-line TEM resonator, FEM and MoM calculations, MRI probe, Frequency response, S-parameters, High Q

1.INTRODUCTION

Magnetic resonance imaging (MRI) systems for medical and scientific applications require a high-performance, high-power inductor capable of establishing a uniformly strong magnetic field. The transverse electromagnetic (TEM) resonator [1-4] has received a great deal of attention as a superior replacement for standard birdcage coils [5] in MRI applications requiring magnetic field levels of 4.7 to 9.4 T. For example, in references [1, 6-7] it has been demonstrated that at operating frequencies of 200 and 400 MHz, a TEM resonator can achieve better magnetic field homogeneity and a higher quality factor Q_0 than an equivalent birdcage coil resulting in improved MRI image quality.

The primary difference between a TEM resonator and a birdcage coil is the cylindrical shield. The shield functions as an active element of the system, providing a return path for currents in the inner conductors. In a birdcage coil, the shield is a separate entity, disconnected from the inner elements, and only reflecting the fields inside the coil to prevent excessive radiation loss. Because of its shield design, a TEM resonator behaves like a longitudinal multiconductor transmission line that can support standing waves at high frequencies [8]. Unlike a birdcage coil, the TEM resonator's inner conductors do not possess connections to their closest neighbors, but instead connect directly to the shield through capacitive elements. Resonance mode separation is accomplished though mutual coupling between the inductive inner conductors. Since all the conductors connect to the shield with tunable capacitive elements, the field distribution can be adjusted to achieve the best homogeneity.

In this work we are interested to analyze and design n-element unloaded coupled-microstrip-line TEM resonator for MRI applications using two approaches based on the use of the finite element method (FEM) and the method of moments (MoM).

Our numerical models allow the determination of the inductive and capacitive matrices respectively [L] and [C_0] with respect to the geometrical parameters of the unloaded TEM resonator.

To demonstrate these numerical methods, a twelve-element unloaded coupled-microstrip-line TEM resonator will be designed and analyzed. The resonator has -118 dB minimum reflection and an unloaded quality factor Q_0 very superior to 500 at 200 MHz.

2.COUPLED-MICROSTRIP-LINE TEM RESONATOR AND ELECTROMAGNETIC PARAMETERS

The coupled-microstrip-line TEM resonator is schematically shown in Figure 1. The functional elements of the TEM resonator are n inner coupled microstrip conductors, distributed in a cylindrical pattern and connected at the ends with capacitors to the cylindrical outer shield [8].

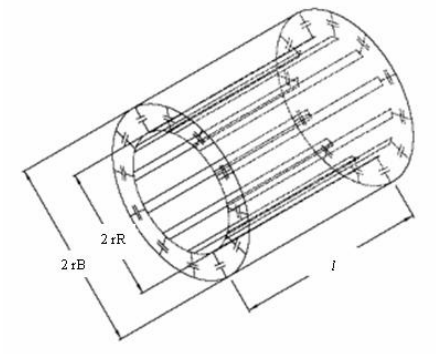

Figure 1: A detailed illustration of the unloaded coupled-microstrip-line TEM resonator.

The cross section of the coupled-microstrip-line TEM resonator is presented in Figure 2. It is formed by an outer shield of radius rB and n microstrip conductors w wide and t thick which constitute the cylindrical pattern of radius rR.

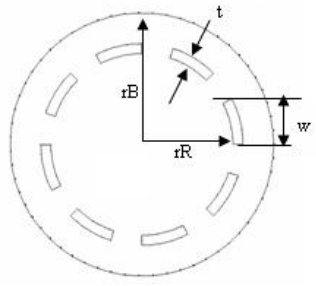

Figure 2: Cross-sectional view of the coupled-microstrip-line TEM resonator (n=8).

The electromagnetic parameters of the coupled microstrip line TEM resonator can be described in terms of its primary parameters [L], [C_0] and its secondary parameter, the unloaded quality factor Q_0.

Where:

$$[L]=\begin{bmatrix} L_{11}.....L_{1n} \\ . \\ . \\ . \\ L_{n1}.....L_{nn} \end{bmatrix} \qquad [C_0]=\begin{bmatrix} C_{11}.....C_{1n} \\ . \\ . \\ . \\ C_{n1}.....C_{nn} \end{bmatrix}$$

The inductance matrix [L] contains the self-inductances of the n-element on the diagonal, and the mutual inductances between elements in the off-diagonal terms.

Matrix [C_0] accounts for the capacitative effects between the n-element, characterizing the electric field energy storage in the unloaded coupled-microstrip-line TEM resonator.

The coefficients for these matrices are obtained by solving a two-dimensional static field problem using FEM [9], [10] and MoM methods [11].

For the FEM approach, the solution is obtained by solving the Laplace's equation (Figure 3-a):

$$\text{div}\,[\nabla_t V(x,y)] = 0 \qquad (1)$$

subject to:

V = 1Volt on the i^{th} conductor's surface.

V = 0 on all others conductors.

This solution represents the distribution of the potential V at the different mesh nodes of the MRI resonator (Figure 3-b).

When the potential V is known, we calculate the i^{th} row of the [C_0] matrix from the electric charge on each conductor.

$$C_{0\,ij} = (1/V_0) \int_{lj} q_s \, dl \qquad (2)$$

Where V_0 = 1Volt, $q_s = \varepsilon_0 \varepsilon_r E_N$; ($\varepsilon_r$ =1), lj represents the contour around the j^{th} conductor and E_N is the normal component of the electric field.

In the high-frequency limit, i.e. the skin depth is sufficiently small such that current flow occurs only on the surface of the conductors, the inductance matrix [L] can be obtained from the matrix [C_0] [8], [10]. The inductance matrix in terms of [C_0] is:

$$[L] = \mu_0 \varepsilon_0 [C_0]^{-1} \qquad (3)$$

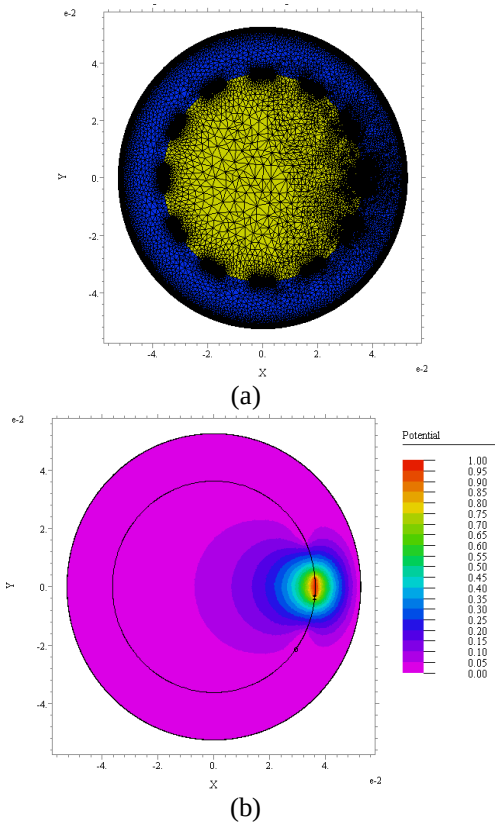

(a)

(b)

Figure 3:FEM meshes on (a) and potential distribution on (b).

For the MoM approach, the numerical calculations of the primary inductive and capacitive matrices ([L] and [C_0]) of the studied resonator were carried out with LINPAR for windows (Matrix Parameters for Multiconductor Transmission Lines), a 2D software for numerical evaluation of the quasi static matrices for multiconductor transmission lines embedded in piecewise-homogeneous dielectrics [11]. The technique used in the program is based on an electrostatic analysis. In this analysis the dielectrics are replaced by bound charges in a vacuum and the conducting bodies are replaced by free charges. A set of integral equations is derived for the charge distribution from the boundary conditions for the electrostatic potential and the normal component of the electric field. The method of moments is applied to these equations, with a piecewise-constant (pulse) approximation for the total charge density and the Galerkin technique. LINPAR for windows can analyse arbitrary planar transmission lines and can also analyse any other structure defined by the user.

For our n-element coupled-microstrip-line TEM resonator, we were obliged to supply the cross section of the structure and all relevant dielectric characteristic including the segmentation by using our programs in FORTRAN (Figure 4).

When the matrices [L] and [C_0] are determined, it is possible to estimate the resonance spectrum S_{11} of the resonator shown in Figure 5 using our programs based on the transmission line method (TLM) [12].

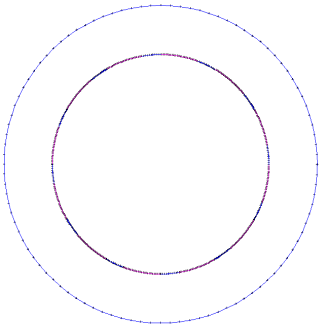

Figure 4: Segmentation of the charged surfaces of the unloaded coupled-microstrip-line TEM resonator.

The MRI probe developed for this article (Figure 5) consists of the 12-element homogeneous coupled-microstrip-line TEM resonator with length *l*, matching capacitor C_M, and terminating capacitors C_{Si} and C_{Li} (i = 1…12).

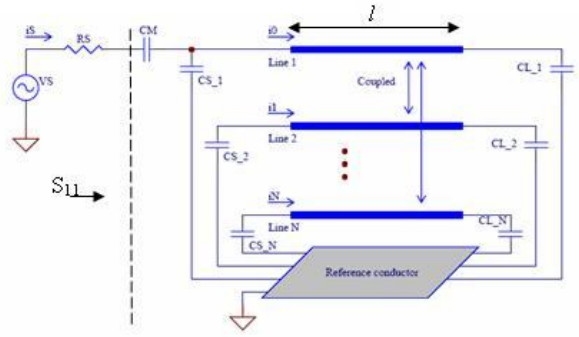

Figure 5: Schematic circuit of the MRI resonator using homogeneous coupled-microstrip-line TEM resonator.

The unloaded quality factor Q_0 of the resonator can be estimated from the reflection-parameter S_{11} sweep with frequency [8], [10]:

$$Q_0 = f_r / (f_u - f_l) \qquad (4)$$

Where:
f_r = the resonance frequency of the circuit,
f_u = 3-dB frequency above the resonance frequency, and
f_l = the 3-dB frequency below the resonance frequency.

3.RESULTS

We applied our coherent FEM and MoM-based numerical tools to the analysis and design of an MRI resonator using 12-element coupled microstrip lines. The FEM and MoM approaches make it possible to simulate the performance of a design and decide if a given set of constraints makes it possible to realize the probe.

To design a MRI resonator operating at 4.7 Tesla (i.e. 200 MHz), we analyzed the structure shown in figure 2 (n = 12). It has twelve inner microstrip conductors and the following set of features:
- Outer cylinder radius: rB = 52.5 mm;
- Inner cylinder radius: rR = 36.25 mm;
- Strip width: w = 6.4 mm;
- Strip thickness: t = 0.038 mm.

The FEM and MoM approaches were employed as shown in Figures 3 and 4 to determine the electromagnetic (EM) parameters of the MRI resonator. As discussed above, the integration of the normal flux over the conductor contours determines the per-unit-length parameter matrices. For example, table 1 lists the first column of the [L] and [C_0] matrices. This information is sufficient to reconstruct the complete matrices since they are circulant [8], [10], [11]. This table shows clearly the good coherence between the results obtained by our two numerical approaches.

\The twelve-element unloaded coupled-microstrip-line TEM resonator can be designed at any resonance frequency for MRI applications, using the EM parameters values presented below.

Table 1: EM Parameters of the MRI resonator

Colonne	C_0 (pF/m)		L (nH/m)	
	FEM	***MoM***	***FEM***	***MoM***
1	21.51	21.49	563.1	564.1
2	-3.84	-3.89	115.7	116.7
3	-0.66	-0.67	46.2	46.85
4	-0.15	-0.31	25.2	25.86
5	-0.19	-0.20	17.1	17.78
6	-0.15	-0.16	13.7	14.45
7	-0.07	-0.15	12.8	13.52
8	-0.15	-0.16	13.7	14.15
9	-0.19	-0.20	17.1	17.78
10	-0.15	-0.31	25.2	25.86
11	-0.66	-0.67	46.2	46.85
12	-3.83	-3.89	115.7	116.7

Finally, the MRI coupled-microstrip-line resonator shown in Figure 5 was designed with the following features: a resonator length, *l*, of 37.5 cm; a matching capacitor, C_M, with value of 15.48 pF, and source and load terminating capacitors, C_S and C_L, respectively, both with value of 1.16 pF.

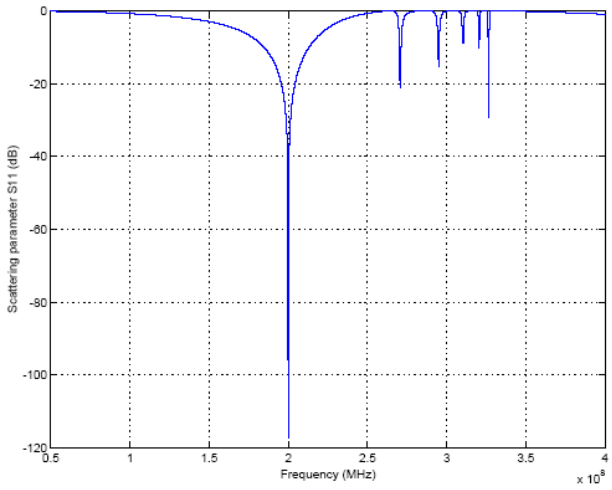

Figure 6: Reverse transmission, S_{11}, at the RF port of the designed MRI resonator.

The simulated frequency response of S_{11} at the RF port of the designed MRI resonator, obtained by our programs based on TLM method, is shown in Figure 6. The curve presents a minimum at the chosen resonant frequency, i.e., 200 MHz. The obtained minimum of reflection for the coupled-microstrip-line TEM resonator is very low at the resonance frequency (-118 dB). Using (4), Q_o was estimated to be very superior to 500.

4. CONCLUSION

This paper presents the analysis and the design of an unloaded twelve-element unloaded coupled-microstrip-line TEM resonator for MRI at 4.7 T (i.e. 200 MHz) which has a high quality factor ($Q_0 > 500$). A finite element method and a method of moment programs have been employed to accurately characterize the electromagnetic parameters ([L] and [C_0]) of the MRI resonator.

When the [L] and [C_0] matrices have been determined, it is possible to simulate the frequency response of S_{11} at the RF port of the designed TEM resonator. This then makes it possible to evaluate the value of the unload quality factor (Q_0) for the MRI resonator. The twelve-element unloaded coupled-microstrip-line TEM resonator is easy to construct, inexpensive, and simple to operate. Furthermore, the coil presented here may be constructed to work at different resonances frequencies, using the EM parameters values presented into this paper.

REFERENCES

1. J. T. Vaughan, H. P. Hetherington, J. O. Out, J. W. Pan, and G. M. Pohost, "High frequency volume coils for clinical NMR imaging and spectroscopy," Journal of Magnetic Resonance Medicine, Vol. 32, pp. 206-218, 1994.

2. P. Röschmann, High-frequency coil system for a magnetic resonance imaging apparatus. US Patent 4746866, 1988.

3. JF Bridges, Cavity resonator with improved magnetic field uniformity for high frequency operation and reduced dielectric heating in NMR imaging devices. US Patent 4751464, 1988.

4. JT Vaughan, Radio frequency volume coil for imaging and spectroscopy. US Patent 5557247, 1996.

5. C. E. Hayes, W. A. Edelstein, J. F. Schenck, O. M. Mueller, and M. Eash, "An efficient highly homogeneous radio-frequency coil for whole-body NMR imaging at 1.5 T," Journal of Magnetic Resonance, Vol. 63, 1985, pp. 622-628.

6. G. Adriany, JT Vaughan, P. Andersen, H. Merkle, M. Garwood, K. Ugurbil, Comparison between head volume coils at high field. In: Proceedings of 3rd SMR and 12th ESMRMB annual meeting, Nice, France, 1995. p 971.

7. J. W. Pan, J. T. Vaughan, R. I. Kuzniecky, G. M. Pohost, and H. P. Hetherington, "High resolution neuroimaging at 4.1 T," Journal of Magnetic Resonance Imaging, Vol. 13, 1995, pp. 915-921.

8. G. Bogdanov and R. Ludwig, "A Coupled microstrip line transverse electromagnetic resonator model for high-field," Journal of Magnetic Resonance Medicine, Vol. 47, 2002, pp. 579-593.

9. N. Ben Ahmed and M. Feham, "Design NMR probes at high frequencies," Microwaves & RF, February 2002, pp. 77-103.

10. N. Ben Ahmed, M. Feham, and M'. Khelif, "Analysis and design of a coupled coaxial line TEM resonator for magnetic resonance imaging," Journal of Physics in Medicine and Biology, Vol. 51, April 2006, pp. 2093-2099.

11. A.R. Djordjevic, D. Darco, M.C. Goran and T. Sarkan, Circuit analysis models for multiconductors transmission lines, Artech Housse, 1997.

12. R. P. Clayton, Analysis of Multiconductor Transmission Lines, New York: John Wiley; 2008.